Hierarchical Organizations

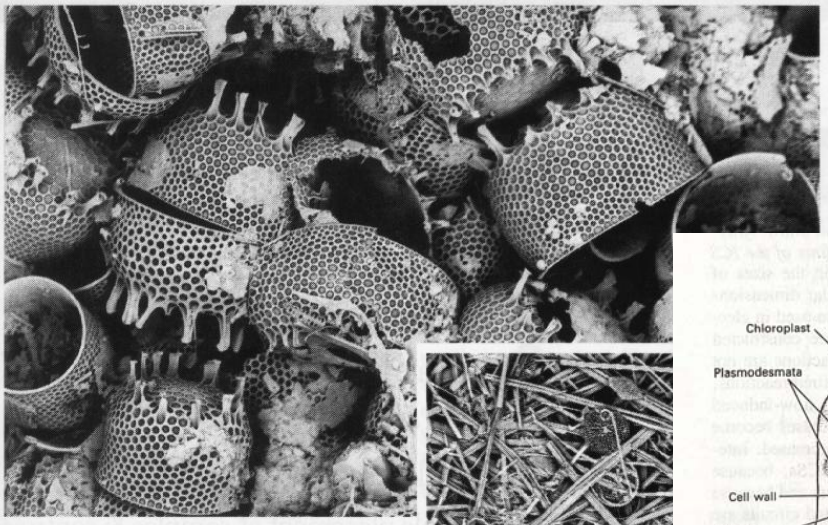

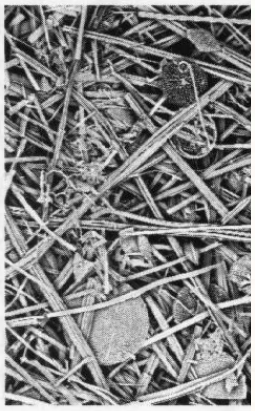

Figure 1 Evidence of the 'fall dump' of giant diatoms identified by Kemp *et al.*[1]. Above, a sediment layer from the Gulf of California dominated by cell walls of *Stephanopyxis palmeriana* (diameter < 70 μm). Right, a sediment layer from the Southern Ocean, showing a tangled mass of the rod-shaped species *Thalassiothrix antarctica*, which grows up to 4 mm in length. (Courtesy of A. E. S. Kemp.)

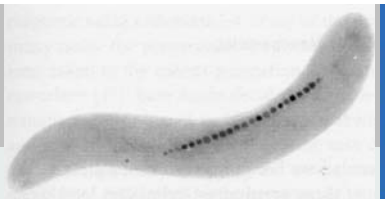

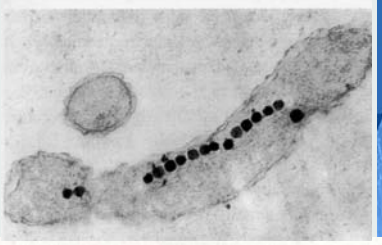

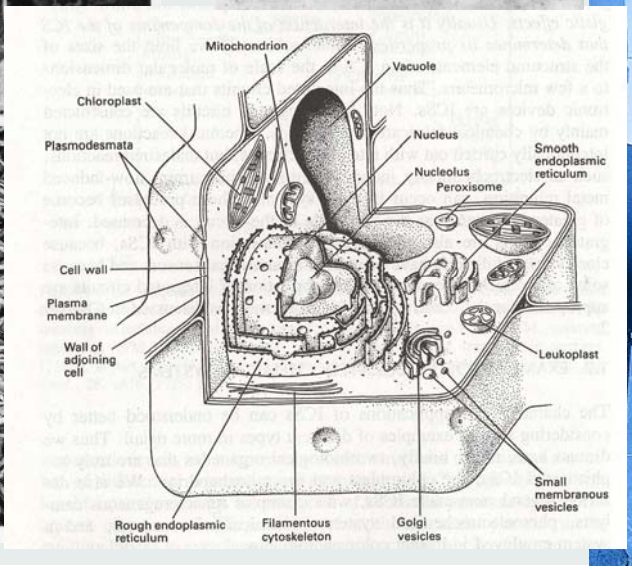

Metals NPs in Solutions and in Polymers

P. Mulvaney, MRS Bull. 2001, 26, 1009

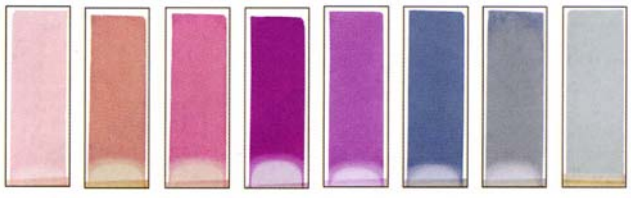

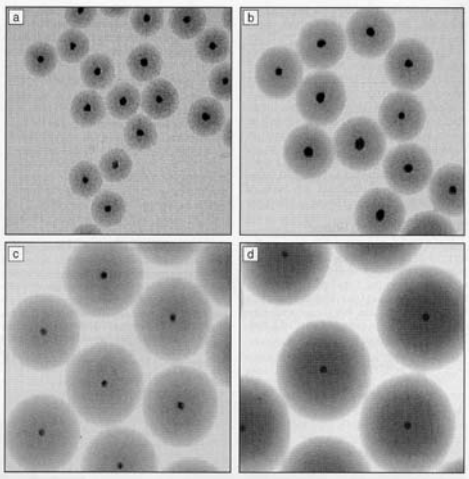

$$R = \frac{(n-1)^2 + k^2}{(n+1)^2 + k^2},$$

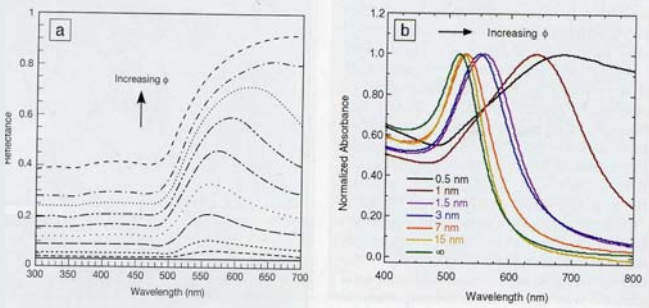

Figure 5. The transmitted colors of a series of gold particle films with decreasing particle spacing. The gold core particles are 15 nm in diameter; the shell thicknesses are, from left to right, 17.5 nm, 12.5 nm, 4.6 nm, 2.9 nm, 1.5 nm, 1.0 nm, 0.5 nm and 0 nm. Films are each 1 cm × 3 cm. The spectra shift smoothly between the two curves shown in Figure 3 as the spacing is varied.[9]

Figure 6. (a) Normalized reflectance spectra for Au@SiO_2 (gold concentrically coated by silica) films as a function of the volume fraction ϕ of Au. From the bottom curve upward, ϕ for each curve, respectively, is 0.01, 0.05, 0.10, 0.20, 0.30, 0.40, 0.50, 0.60, 0.70, and pure Au. (b) The normalized absorbance of a series of Au@SiO_2 films as a function of particle spacing.

Metals NPs in Solutions and in Polymers

P. Mulvaney, MRS Bull. 2001, 26, 1009

Figure 7. Photographs of aligned Ag nanorods in a poly(vinyl alcohol) film. The images shown are the transmitted colors with (a) unpolarized light, (b) horizontally polarized light, and (c) vertically polarized light.

07.11.2006

Fullerenes in CNTs

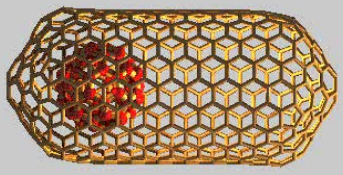

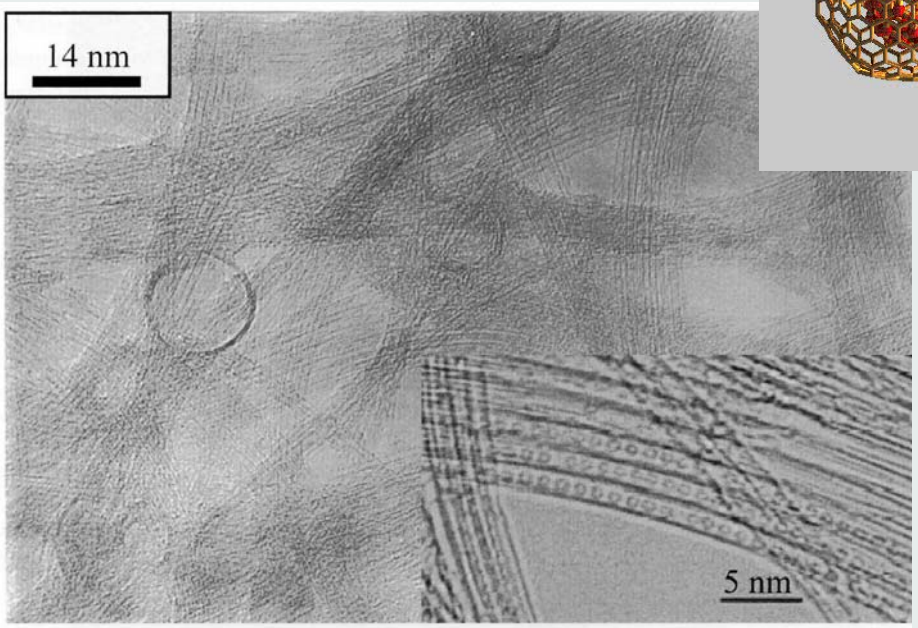

Fig. 8.6. HREM image of SWNTs obtained by arcing graphite electrodes filled with Ni and Y_2O_3 under a He atmosphere (660 Torr). Inset: The HREM image of encapsulated fullerenes inside the SWNTs; scale bar is 5 nm. Reproduced from ref. [45], with permission.

Selforganization of Magnet Colloids

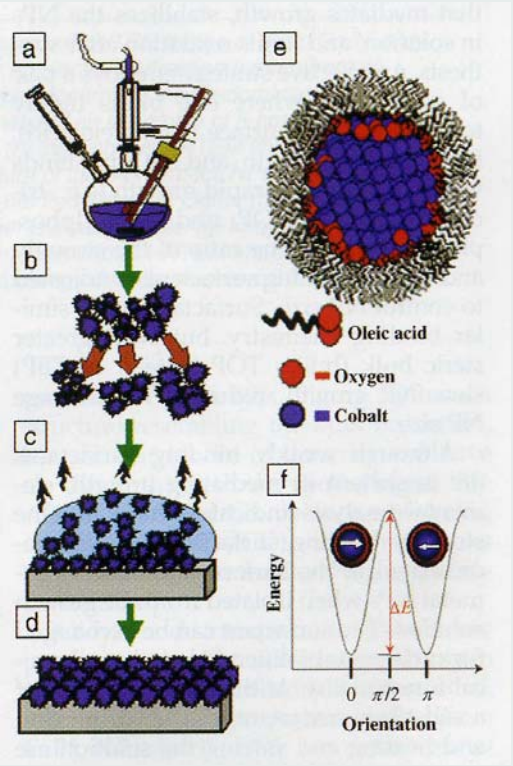

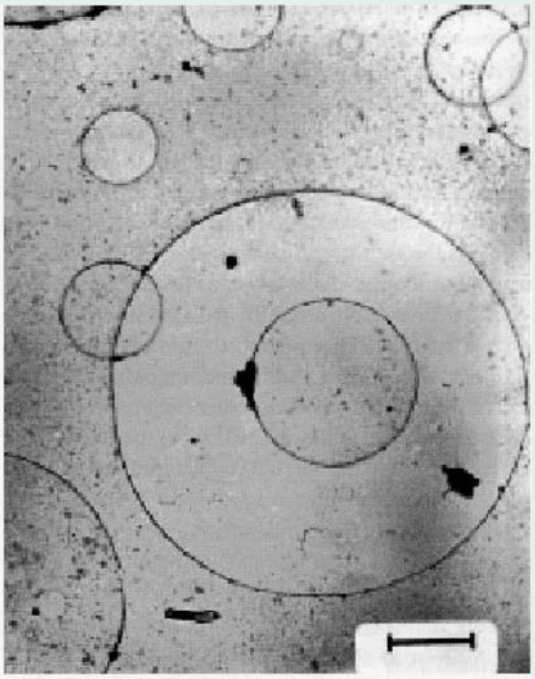

Fig. 6.4. TEM micrograph showing the self-organization of super-paramagnetic nanoparticles into submicron size rings the so-called *Olympic Rings* (scale bar is 0.7 μm).

Hierarchical Crystals from Biomin

Figure 1. Scanning electron micrographs of biogenic calcium carbonate structures: a) Dorsal arm plate of the brittle star *Ophiocoma wendti* with the external array of microlenses. The entire elaborate structure is a single calcite crystal. The lenses are oriented in the optic axis direction of the constituent birefringent calcite. Inset: Epitaxial overgrowth of synthetic calcite crystals on a brittlestar stereom. Note that the nucleation of the newly formed calcite

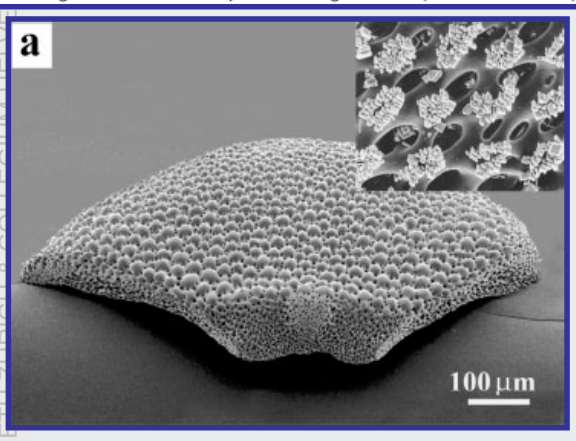

Adv. Mater. 2004, 16, No. 15,

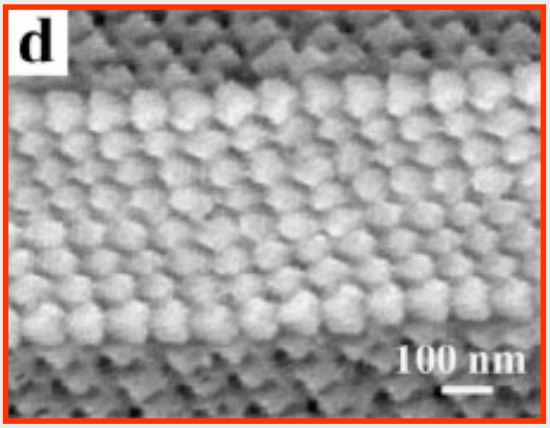

and macromolecules to the local sites of active growth (indicated by arrows). d) Fragment of a coccolith skeleton composed of a highly periodic array of oriented, uniform nanocrystals of calcite.

Super Crystals

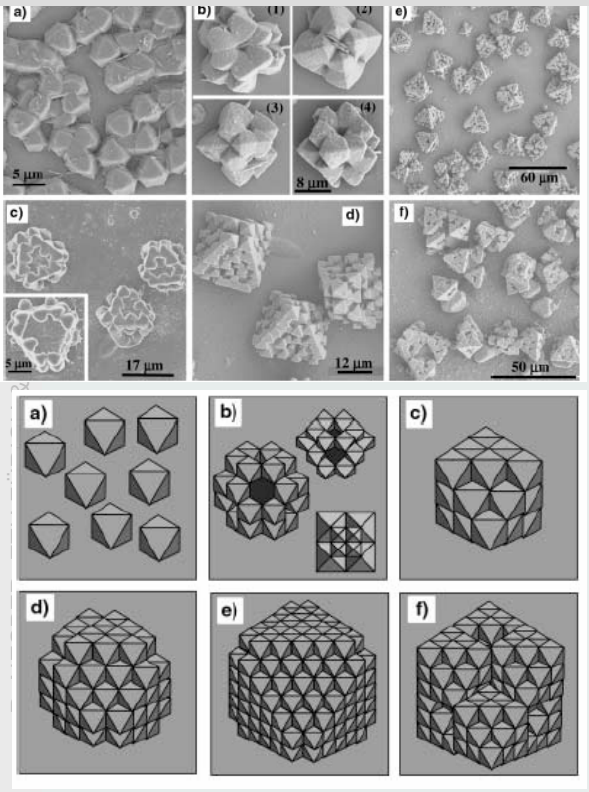

hybrid mesoporous crystals using 1,2-bis(trimethoxy silyl) ethane (BTME) as a silica source and Hexadecyl-trimethylammonium chloride (CTAC) as a surfactant

Angew. Chem. Int. Ed. 2003, 42, 413

Schematic illustrations of edge-sharing stacking:
a) primary octahedral units, face-on configurations,
b) quartet-octahedron modelfor the secondary structure,
c) tertiary structure with filled corners,
d) tertiary structure with unfilled corners,
e) a high-order structure from primary octahedra,
f) a high-order structure from tertiary units.

Principal Forms of Hierarchical Organization

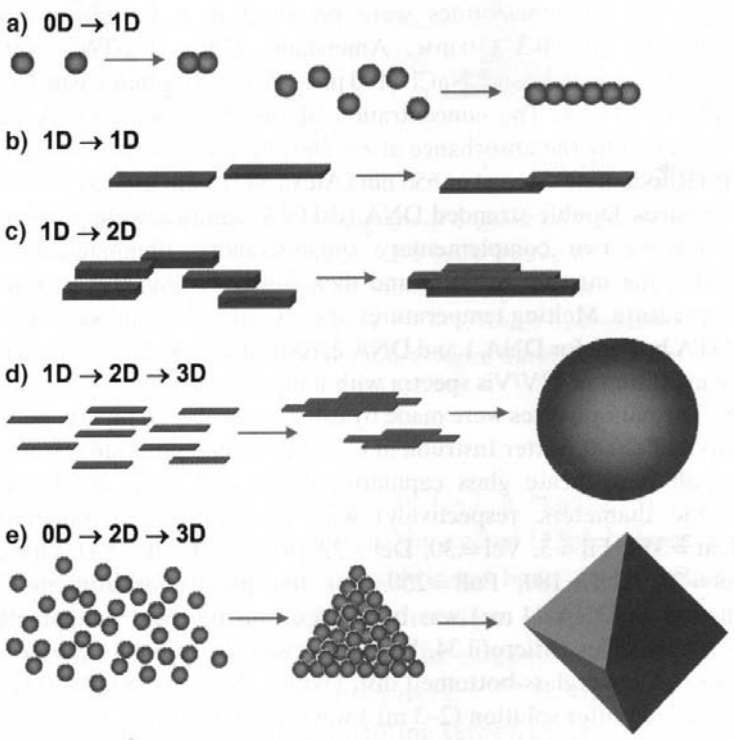

Figure 1. Various organizing schemes for self-construction of nanostructures by oriented attachment.

Metal Cluster Organizations

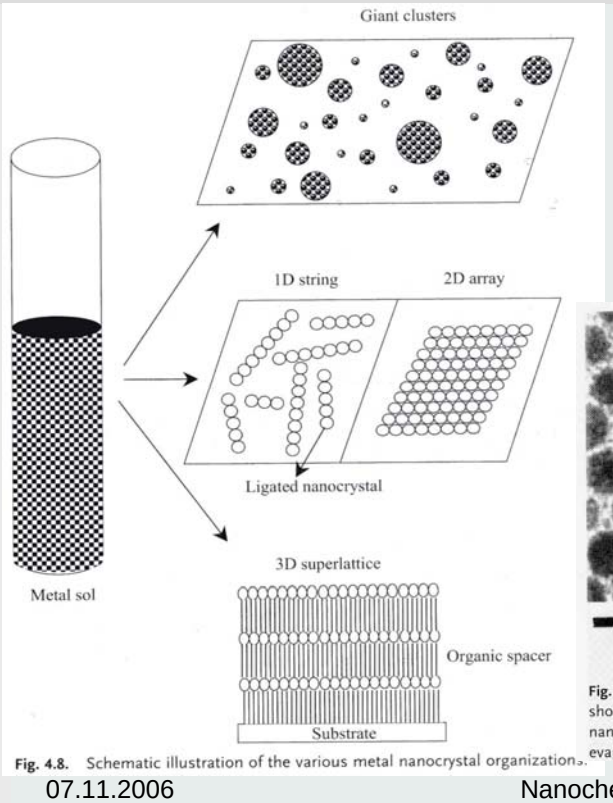

Fig. 4.8. Schematic illustration of the various metal nanocrystal organizations.

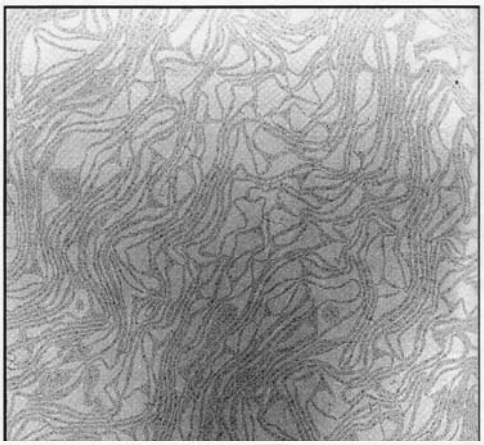

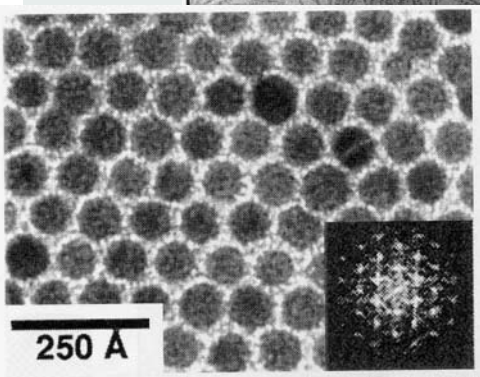

Fig. 4.10. Transmission electron micrograph showing hexagonal close-packed Ag nanocrystals (diameter, 7 nm) obtained by evaporating a chloroform dispersion on a carbon substrate. The average interparticle distance is 1.5 nm. Inset shows the 2D power spectrum of the image (reproduced with permission from [112]).

Metal Cluster Organizations

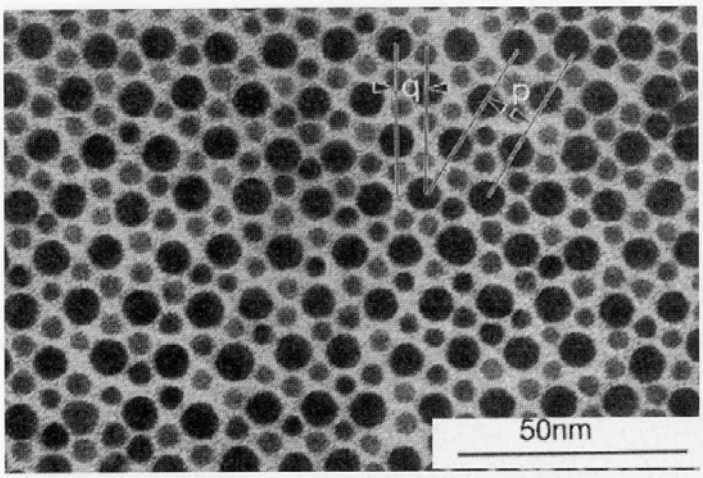

Fig. 4.14. A bimodal hexagonal array of Au nanocrystals. The radius ratio of the nanocrystals is 0.58 (reproduced with permission from [113]).

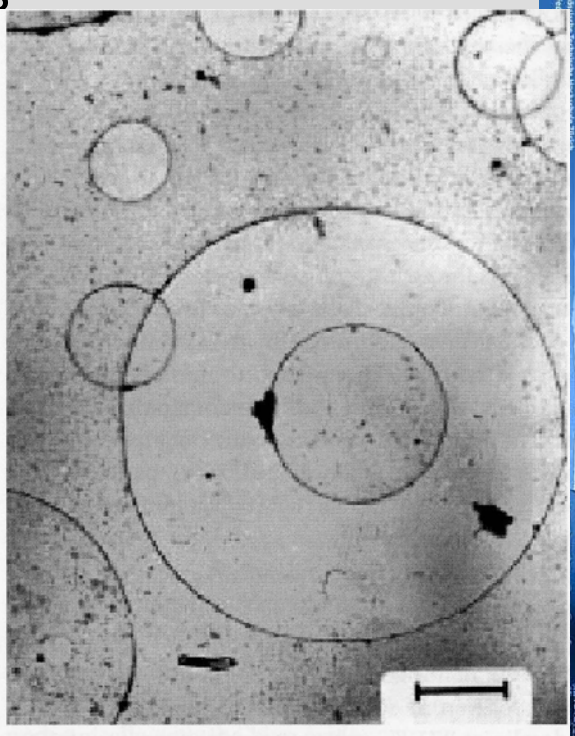

Fig. 6.4. TEM micrograph showing the self-organization of super-paramagnetic nanoparticles into submicron size rings the so-called *Olympic Rings* (scale bar is 0.7 μm).

Super Crystals

Spontaneous ordering of bimodal ensembles of nanoscopic gold clusters

C. J. Kiely*, J. Fink*†, M. Brust†, D. Bethell† & D. J. Schiffrin†

* Materials Science and Engineering, Department of Engineering, The University of Liverpool, Liverpool L69 3BX, UK
† Department of Chemistry, The University of Liverpool, Liverpool L69 7ZD, UK

Nature (1998) 396, 444

primary structure

after aging

phase separation

design – two cluster sizes

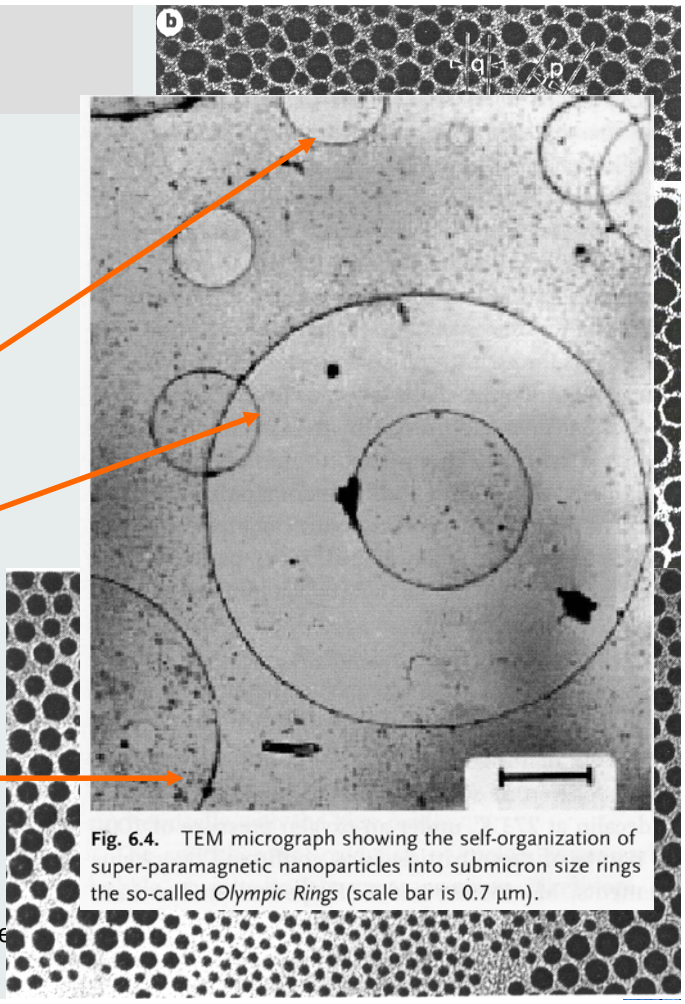

Fig. 6.4. TEM micrograph showing the self-organization of super-paramagnetic nanoparticles into submicron size rings the so-called *Olympic Rings* (scale bar is 0.7 µm).

Hierarchical Crystals from Zeolite Shells

Fig. 1. Schematic illustration for the encapsulation of nano- (I) and micrometer (II) sized particles into discrete hollow zeolite spheres (a_1,a_2) and macroporous zeolite monoliths (b_1,b_2).

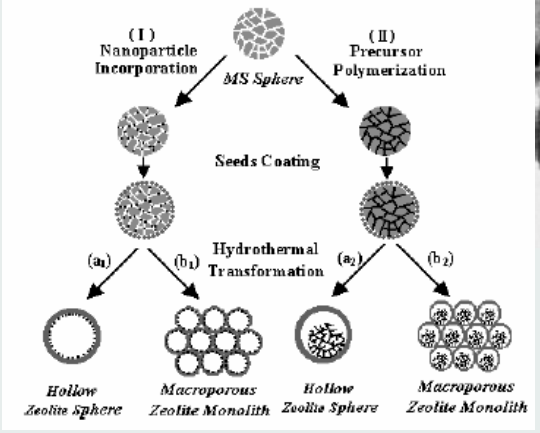

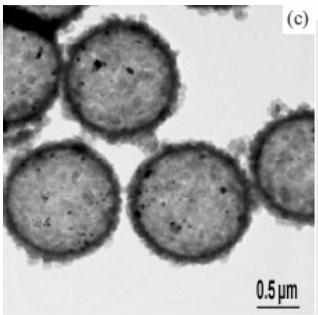

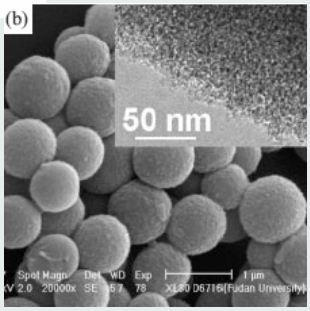

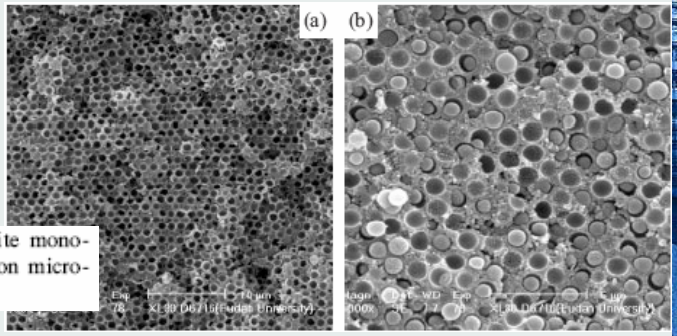

Fig. 7. Cross-sectional SEM images of macroporous zeolite monoliths encapsulated with PdO nanoparticles (a) and carbon microspheres (b).

Adv. Funct. Mater. 2003, *13*,

Selfaggregation and Micro Contact Printing

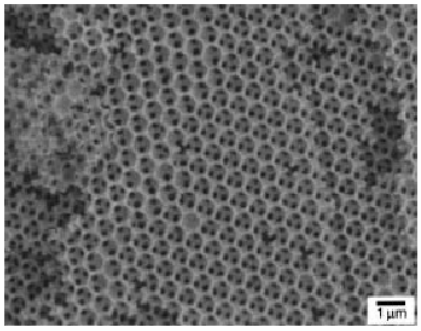

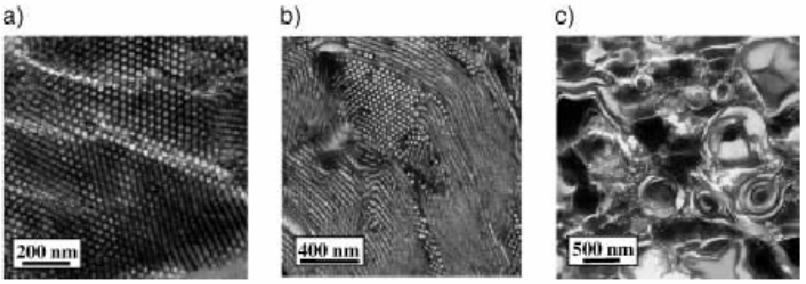

Abbildung 24. Silicate mit a) kubisch geordneten sphärischen Poren, b) hexagonal geordneten zylindrischen Poren und c) lamellaren Poren, hergestellt aus lyotropen Phasen von Blockcolymeren.[95, 134]

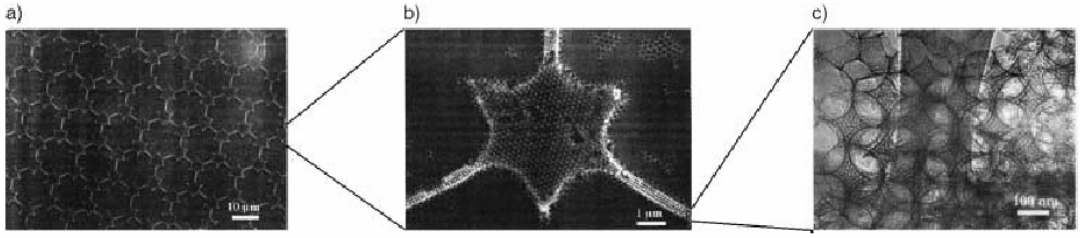

Abbildung 26. Elektronenmikroskopische Aufnahmen einer durch Mikrokontaktdrucken und Selbstanordnung hergestellten Strukturhierarchie über drei Organisationsebenen: a) Mikrokontaktmuster ($d = 15$ µm), b) makroporöse Struktur ($d = 200$ nm), c) mesoporöse Struktur ($d = 2$ nm).[150]

Alignment of Nanotubes and Nanorods

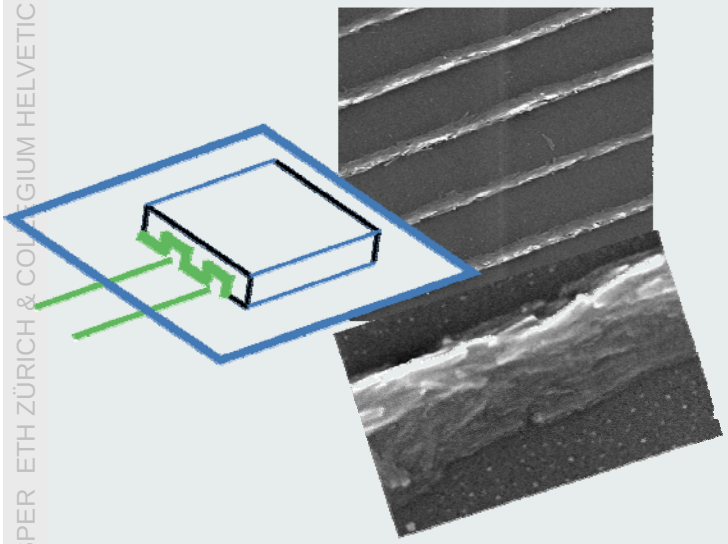

collagene + α–FeOOH composite

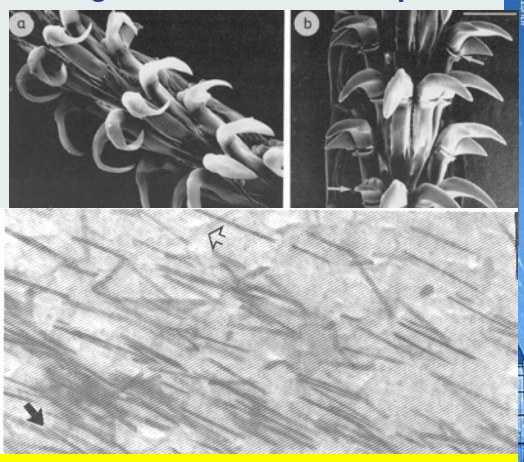

J.Webb, D.J. Macey, S. Mann
in S. Mann, J.Webb, R.J.P.Williams,
Biomineralization, VCH 1989

H.-J. Muhr, F. Krumeich, U. P. Schönholzer, F. Bieri, M. Niederberger, L. J. Gauckler, R. Nesper, *Adv. Mater.* **2000**, *12*, 231-234